

# We are IntechOpen, the world's leading publisher of Open Access books Built by scientists, for scientists

6,900

Open access books available

186,000

International authors and editors

200M

Downloads

Our authors are among the

154

Countries delivered to

TOP 1%

most cited scientists

12.2%

Contributors from top 500 universities



WEB OF SCIENCE™

Selection of our books indexed in the Book Citation Index  
in Web of Science™ Core Collection (BKCI)

Interested in publishing with us?  
Contact [book.department@intechopen.com](mailto:book.department@intechopen.com)

Numbers displayed above are based on latest data collected.  
For more information visit [www.intechopen.com](http://www.intechopen.com)



# Rapid Tooling Development

Sadegh Rahmati

*Islamic Azad University (IAU) – Majlesi Branch  
Iran*

## 1. Introduction

Now a days, rapid prototyping (RP) technology is commonly used to quickly realise the conceptualization of a product design by creating prototypes. These prototypes allow designers and engineers to visualise potential problems, and to implement different solutions in the early product design stages. These prototypes may be used in different industries such as aerospace, aeronautics, automobile, home appliances, industrial equipment, electronic devices, etc. The selection of the suitable RP technique for the manufacturing of a certain product is a very complex problem and depends on several factors (Chen and Cheng, 2000).

Rapid tooling (RT) provides a significant increase in speed and reduction in cost, while for small production runs and complex objects, RP is often the best manufacturing technique available (Ilyas et al., 2010). Moreover, RP, RT and Rapid Manufacturing (RM) techniques can also be used to rapid manufacture parts with excellent quality (Quail et al., 2010; Campbell, et al., 2011). Currently, companies are experiencing increasing pressure to produce complex and diverse products in shorter product development cycles, aiming to achieve less overall cost with improved quality (Evans and Campbell, 2003).

As delivery time and cost of products are on a downward trend, the modern mould manufacturers are increasingly more under pressure to produce moulds quickly, accurately, and at lower cost. Evidently, rapid prototyping and rapid tooling have shortened time to produce a physical prototype or tool. Hence, RP, RT and RM are playing an increasingly significant role in responding to intense global markets competition and achieving compressed time-to-market solutions (Bibb et al., 2009).

In order to investigate the success of rapid tooling technology, two case studies are presented and analysed in this chapter. The first case study is the development of stereolithography (SL) tooling for short run plastic injection mould tooling. The second case study is dealing with development of rapid wax injection mould tooling to be used for investment casting process.

## 2. Stereolithography rapid tooling

In the first case study the development of stereolithography (SL) tooling for short run plastic injection mould tooling is investigated. As manufacturing industry encounters a growing demand for rapid tooling, RP technology in particular stereolithography tooling has demonstrated to have significant potential in product and tool development. However, among different tooling processes, the process of rapid plastic injection mould tooling is

significantly critical for the industry. Compared to still higher resolving techniques, stereolithography bears the advantages of short processing times and good surface finish. Tool makers and manufacturers usually describe the performance of their devices in terms of accuracy or minimal layer thickness, and minimal surface roughness achieved.

Due to the fact that stereolithography has obtained a resolution as high as 60  $\mu\text{m}$ , this significant advance in resolution enables stereolithography to build insert components with improved performance. High performance stereolithography resins, minimum layer thickness of 0.06 mm, minimum surface roughness of 4  $\mu\text{m}$ , and nearly zero shrinkage, has made SL an ideal candidate for rapid tooling purposes. Consequently SL tooling techniques are improving and are becoming increasingly popular among manufacturers (Decelles & Barritt, 1996; Greaves, 1997; Jacobs, 1996).

During the last few years, significant research and developments are achieved by different research groups which have worked on rapid tooling issues. Weiss has demonstrated that a rapid prototype model can be used as a master to get a shell of metal and with a supporting material such as epoxy resin, it can be used for injection moulding, metal forming and EDM electrode (Weiss et al., 1990). Paul Jacobs has discussed the non-homogeneous mechanical property of SL models. He showed that the mechanical property of SLA models are a function of laser exposure and prior knowledge about it can help to reduce the shrinkage generated distortion during part building process and post curing operation (Jacobs, 1992). Gargiulo carried out an experiment with various hatch styles to improve part accuracy of stereolithography (Gargiulo, 1992). Richard discussed the effects of parameters on the accuracy of parts built by SL process (Richard, 1993). Rahmati and Dickens developed a series of experiments to demonstrate the performance of SL rapid tooling to utilise them as injection moulding tools (Rahmati & Dickens, 1997).

In this case study, the SL injection mould has been analysed using different CAE simulation softwares. In particular, MoldFlow is used to get plastic injection moulding parameters such as speed, and pressure. Next, ANSYS software is utilised to investigate the forces exerted on different features of the inserts and to investigate the locations of stress concentration during injection cycle. The result of MoldFlow and ANSYS software analysis demonstrates and confirms the practical results, and assures the possibility of using stereolithography rapid tooling for batch production.

Previous work at Nottingham University has shown that SL injection mould tooling can be used successfully in low to medium shot numbers (Rahmati & Dickens, 2005). Previous work included the tool experimental procedure, testing mechanical properties of the epoxy resin on tensile and impact strength, tool temperatures studies, and tool injection pressure analysis. However, this work is focusing on development of simulation and analysis of SL rapid tooling, where the SL injection mould has been analysed using MoldFlow to get plastic injection parameters such as speed, and pressure. The forces exerted on different features of the insert are calculated and utilised at ANSYS to investigate the stress concentration locations.

## 2.1 Injection pressure analysis

When plastic melt enters the mould cavity, it is normally a flow with an advancing flow front and moving radially away from the centre, while the cavity fills from the gate with the fountain shaped flow front advancing to the opposite end of the cavity and hitting the blocks (Walter & Helmut, 2000; Rauwendaal, 2000). This type of the flow is referred to as fountain flow as it is illustrated in Figure 1. Elements of the fluid in the centre region first

decelerate as they approach the flow front, then the elements start to move tangentially towards the wall. The wall is relatively cold and a frozen skin layer will form behind the advancing flow front.

The elements in the flow front are stretched as they move from the centre towards the wall. The fountain flow mechanism is responsible for a high degree of orientation of the surface layers of the moulded product. This is due to the stretching of the fluid elements approaching the wall while cooling occurs at the wall. The cooling rate is much slower as moving away from the wall and as a result, more relaxation can occur inside the material. Many studies have confirmed significant gradients in orientation and morphology from the outside layers to the inside of injection moulded parts.

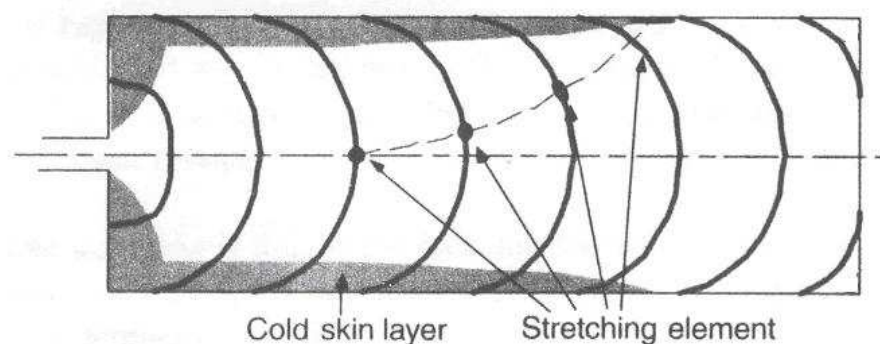


Fig. 1. Illustration of fountain flow into a mould cavity (Rauwendaal, 2000)

The flow loses heat and pressure as it moves away from the centre and in addition to this pressure loss, the flow moving upwards faces additional loss due to the bends. There are two main forces acting on the blocks, one due to the shear stress acting on the base, the other is the bending stress trying to tip over the blocks. In general, at any instant where the injection pressure is higher than the tool strength, failure is feasible. To avoid this, care is taken to inject at a temperature where the tool has sufficient strength. This criteria has led to a well defined cycle, where injection always takes place when the tool temperature has dropped to 45°C, where the material's strength and toughness is able to resist the injection pressure. Stresses exerted on the cavity are dependent on parameters such as melt velocity, and injection pressure.

## 2.2 MoldFlow & ANSYS fundamentals

According to the principle of continuity which is based on the mass conservation, the mass of melt entering at a control volume in unit time is equal to the mass leaving (Fig. 2).

$$\frac{\delta}{\delta t} \int_{c.v} \rho dv + \int \rho \vec{v} \cdot d\vec{A} = 0 \quad (1)$$

Thus the equation of mass conservation by integral is derived. Now the differential presentation of the above is given as:

$$\vec{V} \cdot (\rho \vec{v}) + \frac{\delta \rho}{\delta t} = 0 \quad (2)$$

Here,  $V$  is the velocity of the fluid,  $A$  is the control area,  $\rho$  is mass volume,  $v$  is the control volume,  $p$  is the pressure, and  $t$  is the time. Then the continuity equation is simplified for special case of incompressible fluid ( $\rho = \text{const}$ ).

$$\frac{\delta}{\delta t} \int_{c.v} dv + \int_{c.s} \vec{v} \cdot d\vec{A} = 0 \quad (3)$$

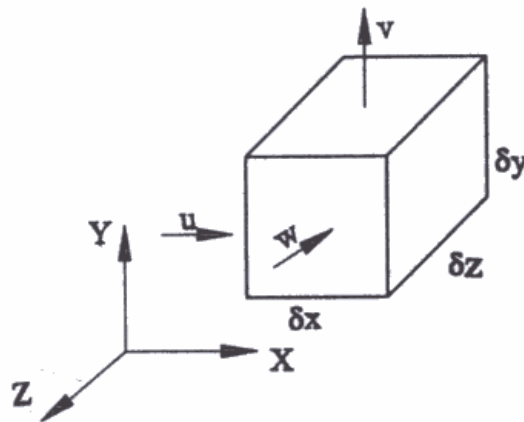


Fig. 2. Rectangular element within the enclosed volume

Integral presentation of the Newton second law of motion is given as follows:

$$\sum \vec{F} = \vec{F}_s + \vec{F}_b = \frac{\partial}{\partial t} \int_{c.v} \vec{v} \rho dv + \int_{c.v} \vec{v} \rho \vec{v} \cdot d\vec{A} \quad (4)$$

This states that the sum of body force and surface force is equivalent to the change of reference volume plus net motion leaving the reference volume. Here,  $F_s$  is the shear force, and  $F_b$  is the normal force.  $\sum F$  is the sum of effective external forces on the reference volume. It is possible to expand this equation in any desired direction. Differential presentation of this equation, assuming  $\rho$  and  $\mu$  to be constant, is known as Navier-Stokes equations. Hence, Euler's equation along the streamline for a steady flow, regardless of volume forces is given as follows:

$$\frac{1}{\rho} \frac{\partial P}{\partial s} = -v \frac{\partial v}{\partial s} \quad (5)$$

When the Euler's equation is integrated along the streamline, Bernoulli's equation is obtained as follows:

$$\frac{P}{\rho} + gz + \frac{v^2}{2} = \text{const} \quad (6)$$

When applying the above equation, one of the two assumptions must be satisfied: equation is given along the streamline, the flow is irrotational. Since the polymer melt flow in the cavity is rotational, thus Euler's equation must be applied along the streamline. Fig. 3

illustrates the flow between two parallel plates at a distance of 'a', where the flow is developed as lamina, steady, and incompressible.

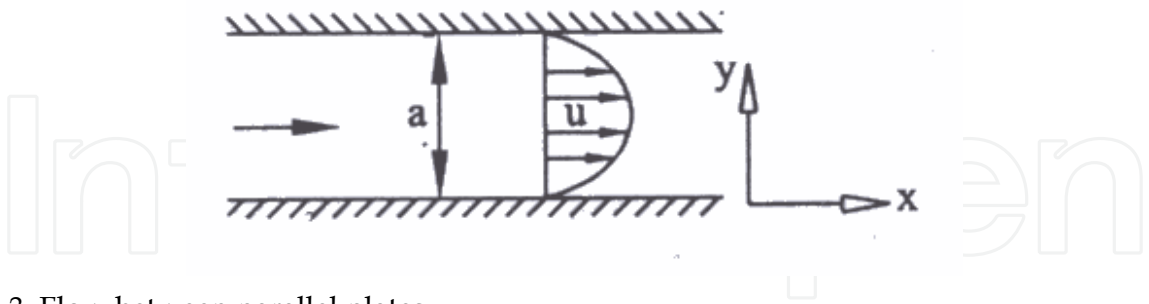


Fig. 3. Flow between parallel plates

Solving the Bernoulli's equation for the above situation, velocity distribution and shear stress distribution for the flow within the parallel plates is obtained.

$$v = \frac{a^2}{2\mu} \left( \frac{\partial P}{\partial x} \right) \left[ \left( \frac{y}{a} \right)^2 - \left( \frac{y}{a} \right) \right] \tag{7}$$

$$\tau_{yx} = \mu \frac{du}{dy} = a \left( \frac{\partial P}{\partial x} \right) \left( \frac{y}{a} - \frac{1}{2} \right) \tag{8}$$

Moreover, flow rate passing within two parallel plates is given as follows:

$$Q = - \frac{1}{12\mu} \left( \frac{\partial P}{\partial x} \right) a^3 = \frac{a^3 \Delta P}{12\mu L} \tag{9}$$

Here  $L$  is the melt path length. Applying the continuity equation, the forces exerted over the cube surfaces (Fig. 4) is calculated as follows:

$$F_n = P_1 A_1 - P_2 A_2 \cos(\Theta) - \rho_1 V_1 A_1 (V_2 \cos(\Theta) - V_1) \tag{10}$$

$$F_s = -P_2 A_2 \sin(\Theta) - w - \rho_1 V_1 A_1 (V_2 \sin(\Theta)) \tag{11}$$

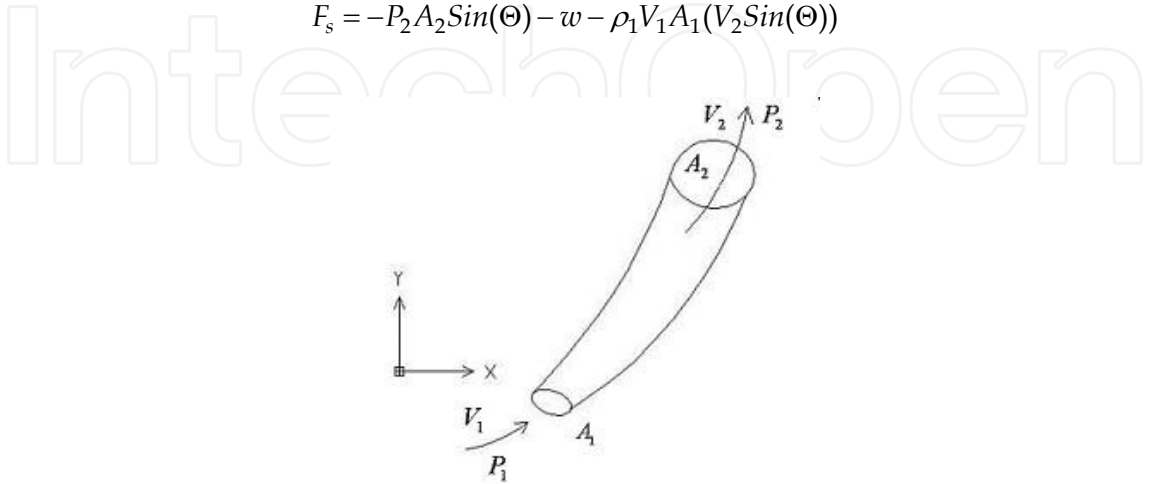


Fig. 4. Schematic representation of flow continuity



Here  $F_n$  and  $F_s$  are the normal force and shear force respectively,  $P_1$  and  $P_2$  are the primary and secondary pressure respectively,  $A_1$  and  $A_2$  are the primary and secondary area respectively,  $V_1$  and  $V_2$  are the primary and secondary velocity respectively, and  $\Theta$  is the melt path angle with respect to horizon.

2.3 Simulation results of MoldFlow

First, the part is designed three dimensionally using the geometrical dimensions shown in Fig. 5. The applied SL injection mould consists of different hollow cubes varying of dimension in the X, Y, and Z axes, i.e. two 10x10x10mm cubes, two 10x9x10mm, two 10x8x10mm, and two 10x7x10mm cubes, all located symmetrically. Then the created 3D model is entered into the MoldFlow software. Next the model is meshed using the FUSION style.

When a 3D volume mesh is created, Moldflow Plastics Insight (MPI) first creates a Fusion mesh from the input file. Then any defects present in the Fusion mesh must be corrected and meshed again using the Generate Mesh dialog. This time, MPI will create the 3D mesh. Fusion works by simulating the flow of the melt on both the top and bottom parts of the mould cavity. Consistency between the results on the opposite sides is maintained by using "connectors" - elements with zero flow and heat resistance. The connectors are inserted automatically at locations determined according to the geometrical features of the model.

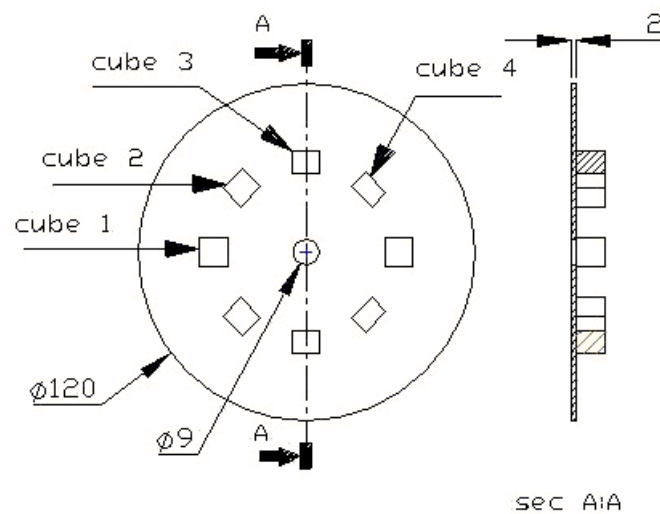


Fig. 5. Geometrical dimensions of the moulding

Next the moulding material is chosen. The material chosen for the MoldFlow analysis has the properties and characteristics, as given in Table 1, and therefore the results of MoldFlow analysis of injection parameters are calculated and presented in Table 1. Now it is possible to analyze the best choice for sprue location, which the result is presented in Fig. 6 in color. As shown in Fig. 6, the best gate location as expected is at the middle of the moulding. After deciding on the gate best location, FILL analysis is carried out.

Material data:	POLYPROPYLENES (PP)
Material structure:	Crystalline
Melt density:	0.72848 g/cm <sup>3</sup>
Solid density:	0.90628 g/cm <sup>3</sup>
Specific heat (Cp):	3000.0000 J/kg-C
Thermal conductivity:	0.1500 W/m-C
Fill time:	2.1000 s
Cooling time:	20.0000 s
Velocity/pressure switch-over:	Automatic
Packing/holding time:	10.0000 s

Table 1. Moulding material properties and injection parameters results

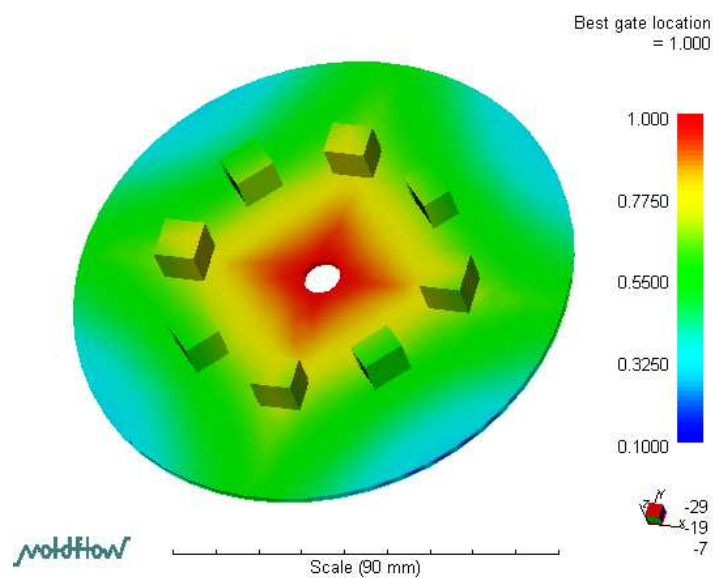


Fig. 6. MoldFlow analyses for sprue bush location

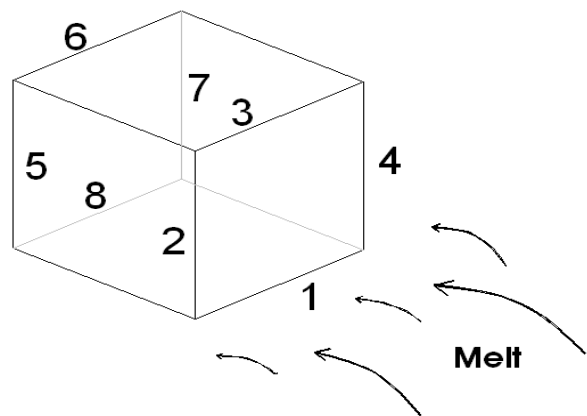


Fig. 7. The identification number of each edge of a cube



The purpose of the FILL analysis is to investigate the pressure and velocity for choosing interested location for cavity. Therefore the result of the FILL analysis about Time at the end of filling is 2.4184s and Total moulding weight is 20.4960 and required clamping force is 13.9166 tones. Comparing the filling time of 2.2 sec resulted from FUSION mesh in Table 1, with the result of FILL analysis of 2.4184 sec, 0.2184 sec difference is due to the fact that FILL analysis has taken the mass of melt including the sprue bush.

Next, the velocity at the edge of the cubes as identified in Figure 7, is analysed. The melt velocity at different cube locations is presented in Table 2 in terms of cm/sec. Due to the fountain effect of melt flow into the cavity, the maximum melt velocity is randomly assigned to one of the cubes in each run of the FILL analysis. However, in order to account for the critical situation, the velocity on edge 8 is assumed to be zero, because the failure may happen while there is a maximum differential pressure build up between the front side and back side of the cubes.

Edge	1	2	3	4
Velocity	91.56	48.38	88.59	98.64
Edge	5	6	7	8
Velocity	14.52	76.5	65.36	19.3

Table 2. Velocities of all edges of a cube in cm/sec

According to the fountain flow behavior of the polymer melt into the cavity, velocities are determined as shown in the Table 2. It is observed that on edge 4 (Fig. 7) which the melt front hits first, the velocity is maximum, while the velocity on the other edges is less. Subsequently, the pressure at all cube edges is determined as in the Table 3 in terms of MPa.

	cube1	cube2	cube3	cube4
Edge1 (MPa)	15.89	16.63	16.25	14.91
Edge2 (MPa)	15.21	15.96	15.73	14.55
Edge3 (MPa)	15.03	15.71	15.36	14.05
Edge4 (MPa)	15.53	16.07	15.57	14.02
Edge5 (MPa)	14.34	15.19	15.28	14.12
Edge6 (MPa)	14.38	15.11	14.9	13.65
Edge7 (MPa)	13.11	15.39	14.97	13.54

Table 3. Pressure of all edges of a cube in MPa

Pressure gradients exerted on each surface is derived from the pressure changes of its edges. Due to the fact that larger surface refers to the bigger cube; subsequently larger pressure changes are expected to happen on bigger cube as well. Accordingly, decreasing pressure

differential trend is expected on the subsequent cubes. Now, with regard to the results obtained from the MoldFlow software and the following fluid dynamics relationships, the forces exerted on each cube is extracted.

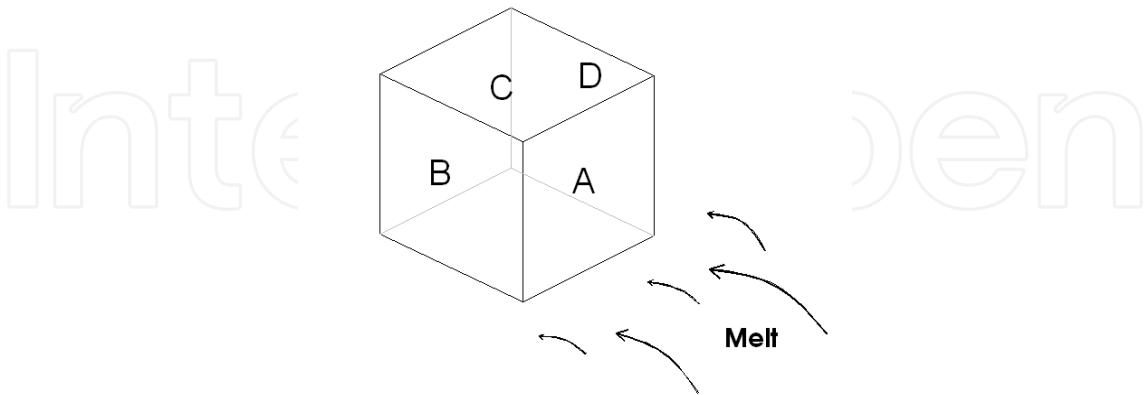


Fig. 8. The identification number of each face of a cube

Due to the fact that only the critical situations are of interest in this analysis, therefore only the maximum differential pressures have been taken into consideration, as presented in Table 4. This table is presenting the normal and shear forces ( $F_n$ ,  $F_s$ ) which exists on the cube surfaces shown in Figure 8, where surface "A" is the front face, surface "B" is the left side face, surface "D" is the right side face, and surface "C" is the top face of the cube.

CUBE1	A	B	C	D
$F_n$ (N)	266.08	255.36	0	257.12
$F_s$ (N)	224.8	225.92	218.4	209.76
CUBE2	A	B	C	D
$F_n$ (N)	232.82	223.44	0	224.98
$F_s$ (N)	196.7	197.68	191.1	183.54
CUBE3	A	B	C	D
$F_n$ (N)	199.56	191.52	0	192.84
$F_s$ (N)	168.6	169.44	163.8	157.32
CUBE4	A	B	C	D
$F_n$ (N)	166.3	159.6	0	160.7
$F_s$ (N)	140.5	141.2	136.5	131.1

Table 4. Forces exerted on each surfaces of cubes (N)

2.4 Simulation results of ANSYS

Now considering the forces obtained from fluid analysis, the core side of the mould is analyzed using ANSYS software for stress investigation. Due to the fact that the mould is designed to be symmetric (Fig. 5), therefore the ANSYS analysis is carried out only for half of the tool (Fig. 9). The 3D model generated, is entered into the ANSYS software. Next the model is meshed using the SOLID95 style which is compatible with three dimensional displacements resulted from the force exerted by melt pressure. SOLID95 mesh is three dimensional and is able to monitor any displacements. In addition SOLID95 elements have

compatible displacement shapes and are well suited to model curved boundaries. The element is defined by 20 nodes having three degrees of freedom per node: translations in the nodal x, y, and z directions. The element may have any spatial orientation. SOLID95 has plasticity, creep, stress stiffening, large deflection, and large strain capabilities.

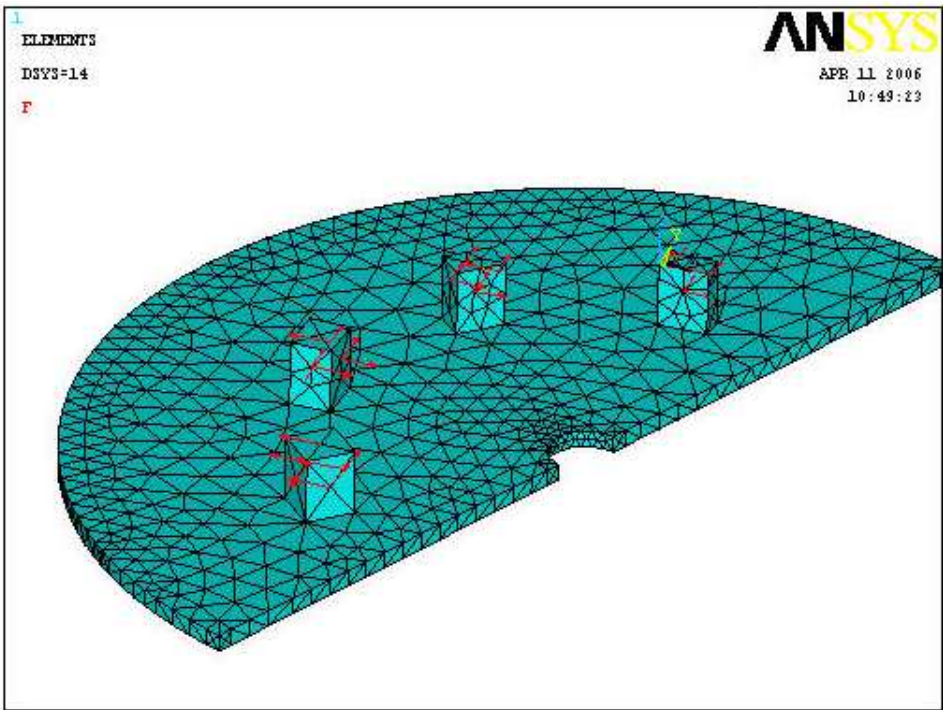


Fig. 9. Half of the core while SILD95 mesh is applied

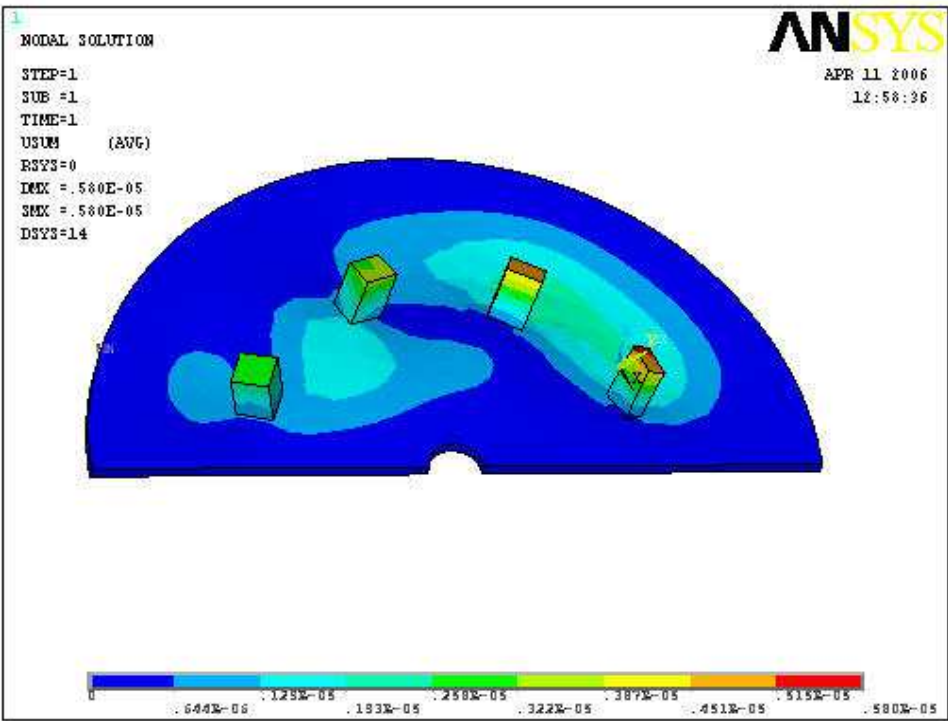


Fig. 10. Displacement analysis of the core

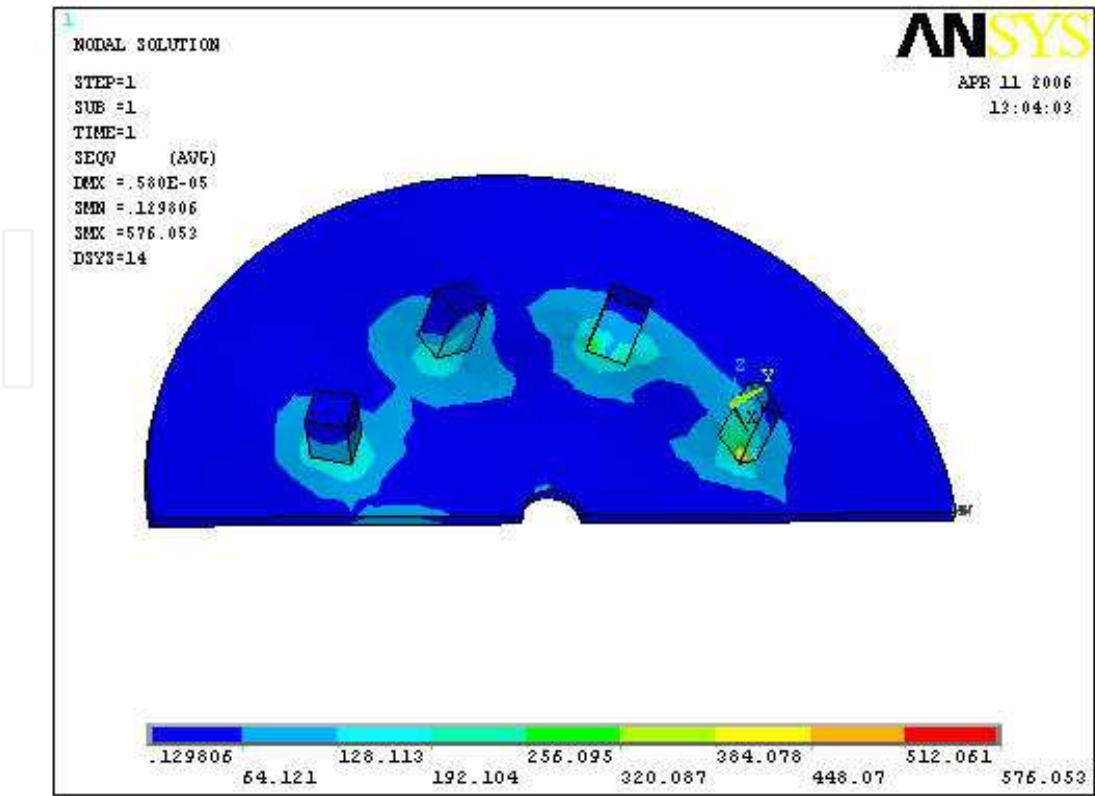


Fig. 11. Von-Mises stress analysis of the core

While the starting conditions of normal forces ( $F_n$ ) and shear forces ( $F_s$ ), as well as boundary conations around the core, are applied, next, the exerted forces are applied at different nodes. In addition, displacements around the core are defined in three axes (i.e 3 degrees of freedom). Next the results of analysis are presented and hence the total displacement is investigated as shown in Fig. 10 where the red color region is the sign of maximum displacement or more chances of failure on the smallest cubes.

2.5 Summary of stereolithography rapid tooling

Evidently, product diversity, high product complexity, increase in product variety, and shorter product life are prime motives for SL tooling development. Due to the fact that many moulding parameters inside the cavity such as net pressure on the mould features, melt velocities at different points, etc. are not possible to be measured, therefore CAE simulation softwares are unique and inexpensive alternatives to analyse and evaluate different rapid tools.

Obviously those CAE simulation softwares such as MoldFlow and ANSYS are significant aids in rapid tooling analysis, acquiring tooling parameters and melt behavior in the cavity; and it is a promising technique for today’s rapid tooling analysis of different SL tooling techniques which have been developed and are complementary for each other.

The experimental results of tool failure on one hand, and simulation results of MoldFlow and ANSYS on the other hand, have good correlation in particular about the first failure which happened on the smallest cube.

As shown from Fig.11, stress generated is maximum on the smallest cube, hence the chances of failure is the most, relative to other cubes.

Design of SL rapid tools must be in such a way that while controlling the stress, the maximum stress exerted on cubes must resist tensile and bending stresses. SL rapid tools having very narrow ribs and fragile features are not recommended with such SL tooling method.

**3. Rapid wax injection tooling for investment casting**

In the second case study, rapid wax injection mould tooling to be used for investment casting process is being developed. Investment casting process is considered as an economic approach in mass production of metal parts with complex shapes using different material alloys. In order to produce wax models for investment casting process, usually conventional tools manufactured via machining process are being used. On the other hand, using conventional tooling for wax model production may lead to extra time and cost, resulting in reduction of overall throughput and reducing the benefit of using such approach particularly for batch production. Rapid prototyping technology and its downstream applications in rapid tooling can lead to significant reduction in time and cost of design and production (Rosochowski & Matuszak, 2000). One of such applications is direct or indirect production of wax models needed in investment casting industry (Bonilla et al., 2001).



Fig. 12. Shift fork of Peugeot engine gearbox

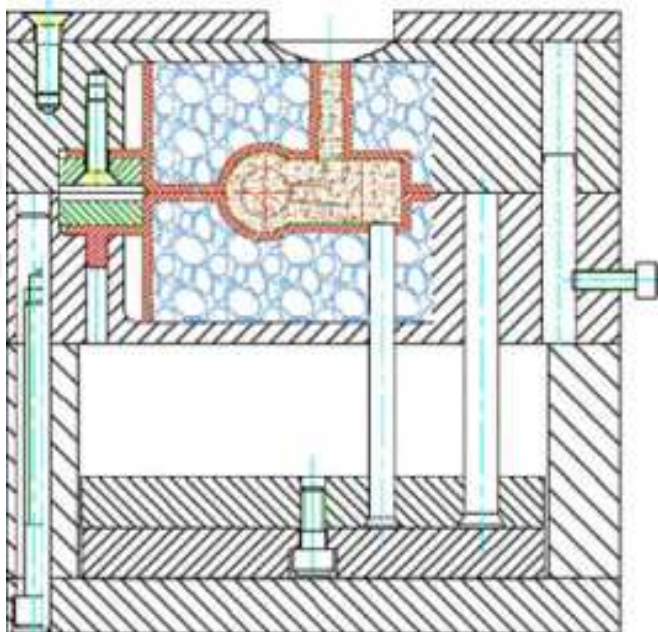


Fig. 13. Wax injection moulding tool of Peugeot engine gearbox shift fork



Applications in wax models demand a kind of processes which are able to produce the final shape and geometry of the part's critical features in near to the net shape with minimum post processing requirements. In this research stereolithography technique is used to fabricate the shell for tool master model of a shift fork of Peugeot engine gearbox (Fig. 12), then this shell is used to make the tool for producing wax model of shift fork via epoxy tooling and direct ACES injection moulding tooling method.

### 3.1 Methodology

In this research, first the 3-D model of the part was created in Catia software. Then, the CAD model of the shift fork was analyzed using MoldFlow to investigate the ideal and optimum conditions of tool operation during wax injection moulding process. In order to construct wax injection moulding tool, epoxy insert shells were fabricated directly from CAD data on an SL machine. These inserts were then fitted into steel mould bases through steel frames accompanied by cooling pipes and were back-filled with aluminum powder/aluminum chip/epoxy resin mixture (Fig. 13). The back-filled mixture added strength to the inserts and allowed heat to be conducted away from the mould.



Fig. 14. Tool assembly components and the steel frames

The modular steel mould bases were two standard base plates machined with a pocket to fit the steel frames and the inserts (Fig. 14) (Menges & Mohren, 1986). Next, vacuum casting machine (MCP 006) was used for creating wax patterns. Experiments were focused on optimization of casting parameters such as wax temperature, vacuum pressure, and mould temperature to achieve better dimensional accuracy of the wax models.

3.1.1 Design of wax model

The first step was creating the specific shape of the product. Therefore, the 3-D model of the part, based on the nominal dimensions, was created in Catia software (Fig. 15). The ideal dimensions are the nominal dimensions plus the shrinkage factors due to the wax material and final casting metal. Therefore, the actual dimensions of the model are the dimensions of the actual casting wax.

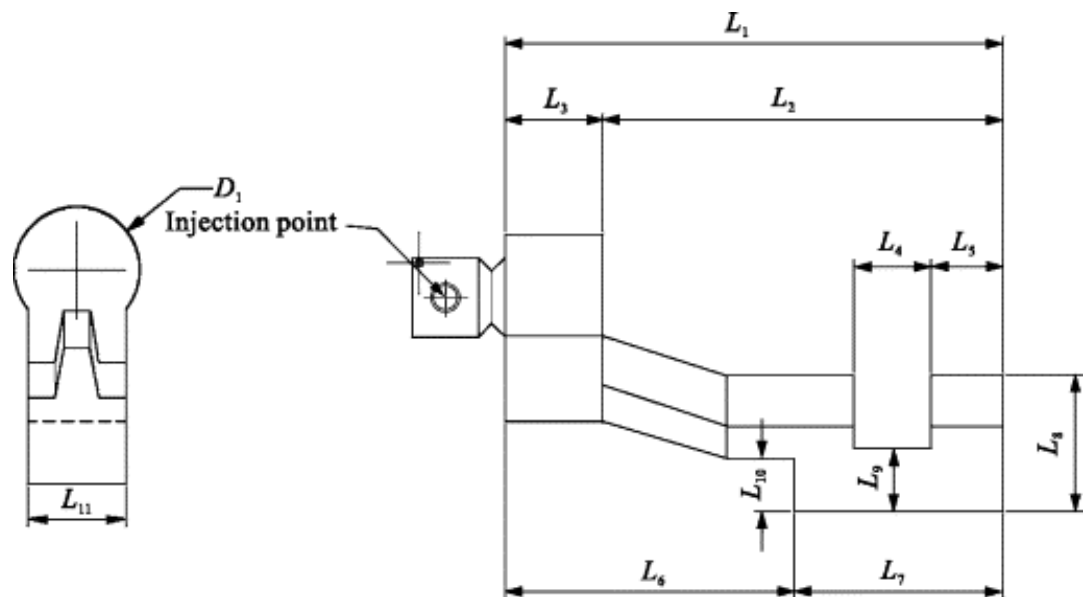


Fig. 15. Wax model parameters

3.1.2 Determination of shrinkage

In traditional moulding, the shrinkages of casting metal and wax material must be considered while creating the mould cavity (Siegfried & Wadenius, 2000). Thus, the mould cavity dimensions should be bigger than the nominal data to compensate the shrinkages of wax and casting metal. The wax shrinkage depends on the thermal conductivity of the mould and the wax solidification rate. Linear shrinkage of the wax could be estimated as follows:

$$S_L = \frac{L_W - L_F}{L_W} \times 100 \tag{12}$$

where  $S_L$  is the linear shrinkage,  $L_W$  is the tool dimension, and  $L_F$  is the wax model dimension. However, if  $\alpha$  is defined as tool expansion coefficient and  $\beta$  as wax expansion coefficient,  $C$  can be defined as the tool actual dimension as follows:

$$L_F = L_W(1 + \alpha), C = L_F(1 + \beta) \Rightarrow C = L_W(1 + \alpha)(1 + \beta) \tag{13}$$



However, in this research the shrinkage of casting metal was determined from casting design handbook and POULADIR Investment Casting Company (Investment Casting, 1968).

### 3.2 Tool simulation and analysis

Computer CAE simulation can reveal tool/model design problems, injection parameters, and difficulties encountered during operation, well before commencing the real operation. In this research, all tool design stages are simulated repeatedly to achieve optimum wax tool performance.

#### 3.2.1 Wax injection process simulation

MoldFlow package was applied to simulate and predict different scenarios and investigate the optimum tool design and injection parameters according to *the MoldFlow User Manual*. Parameters investigated include filling patterns, temperature profiles, residual stresses, tool clamping force centre of gravity, the pressure at different time intervals, tool temperature at any time, and freeze time. Providing correct data input results in appropriate analysis. While providing wax model and tool data to the MoldFlow, the proposed wax data did not exist at the MoldFlow database. Therefore, by consulting MoldFlow Company, a similar wax data from Argueso Company was provided to the MoldFlow database.

Among injection setting parameters, injection time was set at 10 s and freeze time at 30 s. Running different simulations resulted in the most favourable setting appropriate to produce 100 wax models per hour, whereas in conventional tooling these two parameters are 5 s and 10 s, which results in 300 shots per hour. Regarding tool surface temperature determination in MoldFlow, thermal analysis of ANSYS at permanent phase and MoldFlow at the transient phase was conducted according to *the ANSYS User Manual, Version 6.1*.

#### 3.2.2 Simulation results analysis

Problems encountered during actual wax injection process such as weld lines and blush, are determined and corrected by the proper mould design, gate location, and gate design. Fig. 16 indicates air trap spots locations which may occur during wax injection. Fig. 17 indicates weld lines on the wax model where by choosing appropriate gate location, it avoids any weld lines.

Filling process is clearly a complicated process. Fig. 18 indicates the mould filling time of 10.21 s and Fig. 19 indicates the complete melt temperature after the cavity being completely filled to analyze the consistency of uniform temperature distribution of the wax model. Fig. 20 indicates that the freeze time needed for the wax model is 30 s. The injection pressure of the mould cavity is 0.5 MPa.

### 3.3 Wax tool fabrication

For fabrication of the insert cavity using stereolithography machine, the 3-D CAD model from Catia software was corrected by applying the shrinkage values of wax and metal casting to the nominal dimensions. Then, the final CAD wax model was converted into STL format by 3-D Lightyear software. STL is a standard format in RP industries which approximates 3-D-model surfaces with several triangle facets. After implementation of some complementary actions on the STL model, like model review, defining supports, and build orientation, the final CAD file was sent to rapid prototyping apparatus. In this project, insert

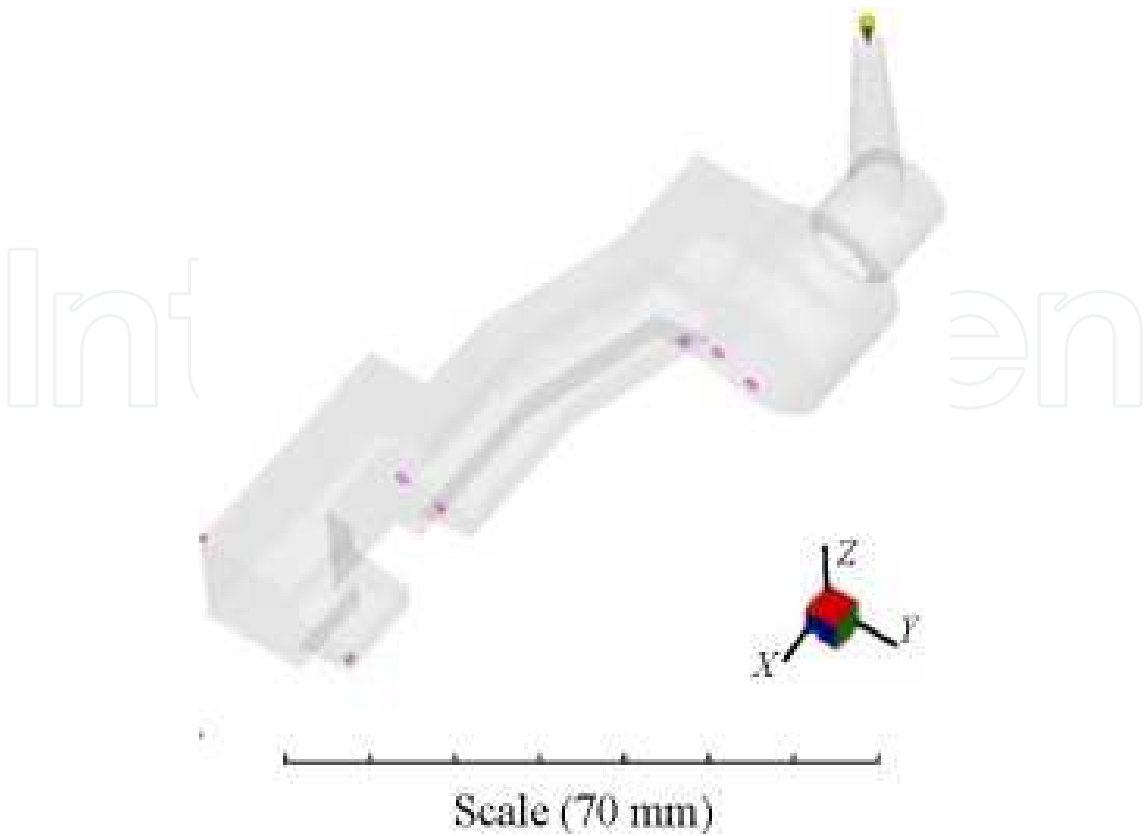


Fig. 16. Air trap spots locations

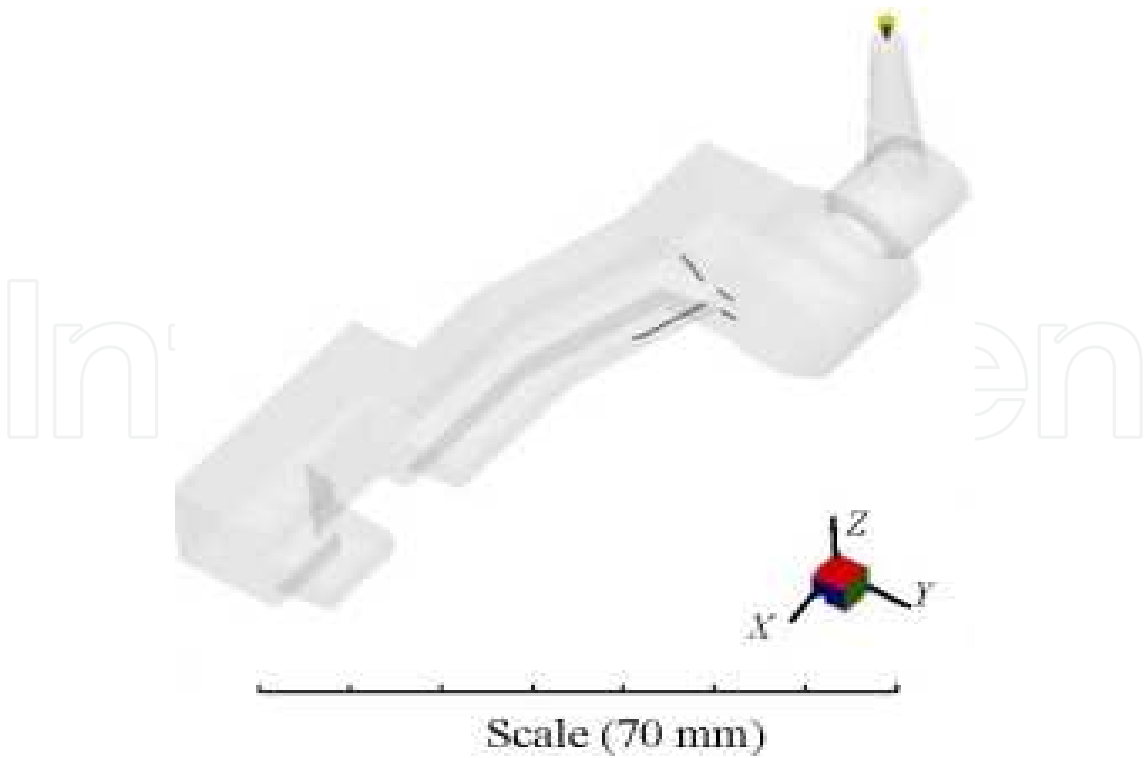


Fig. 17. Wax model weld lines

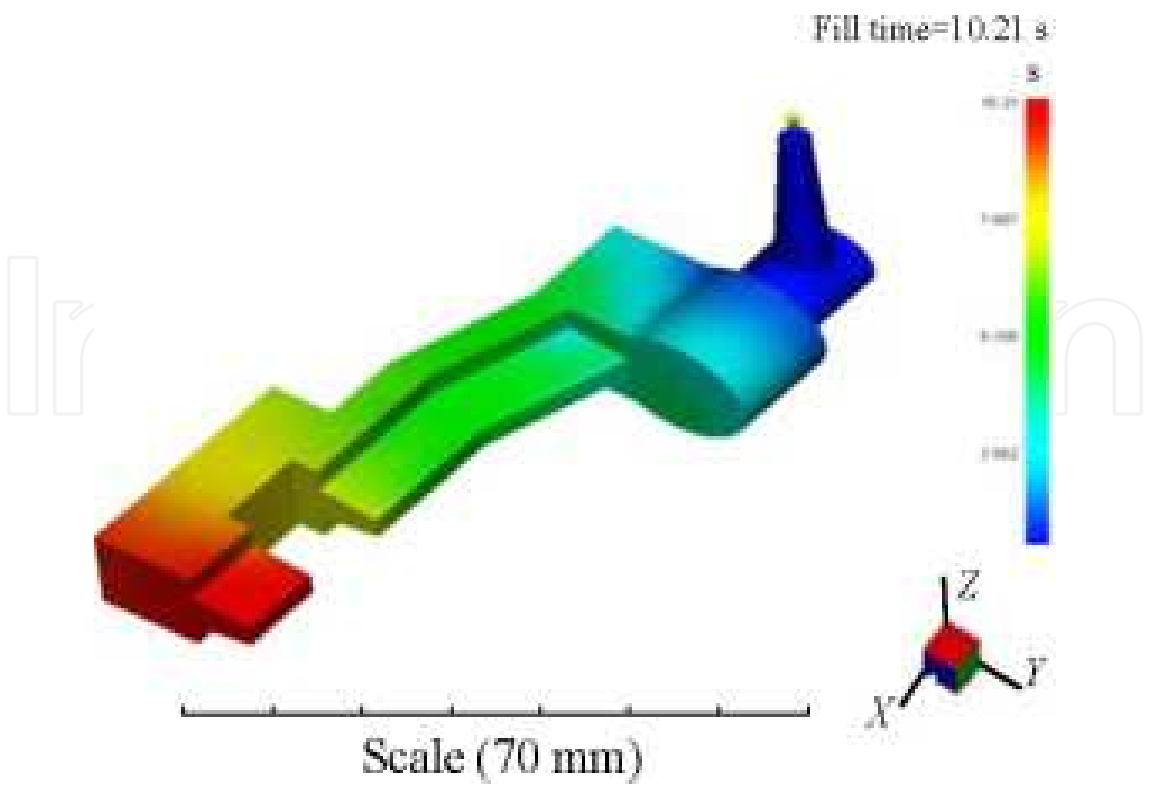


Fig. 18. Wax model filling time

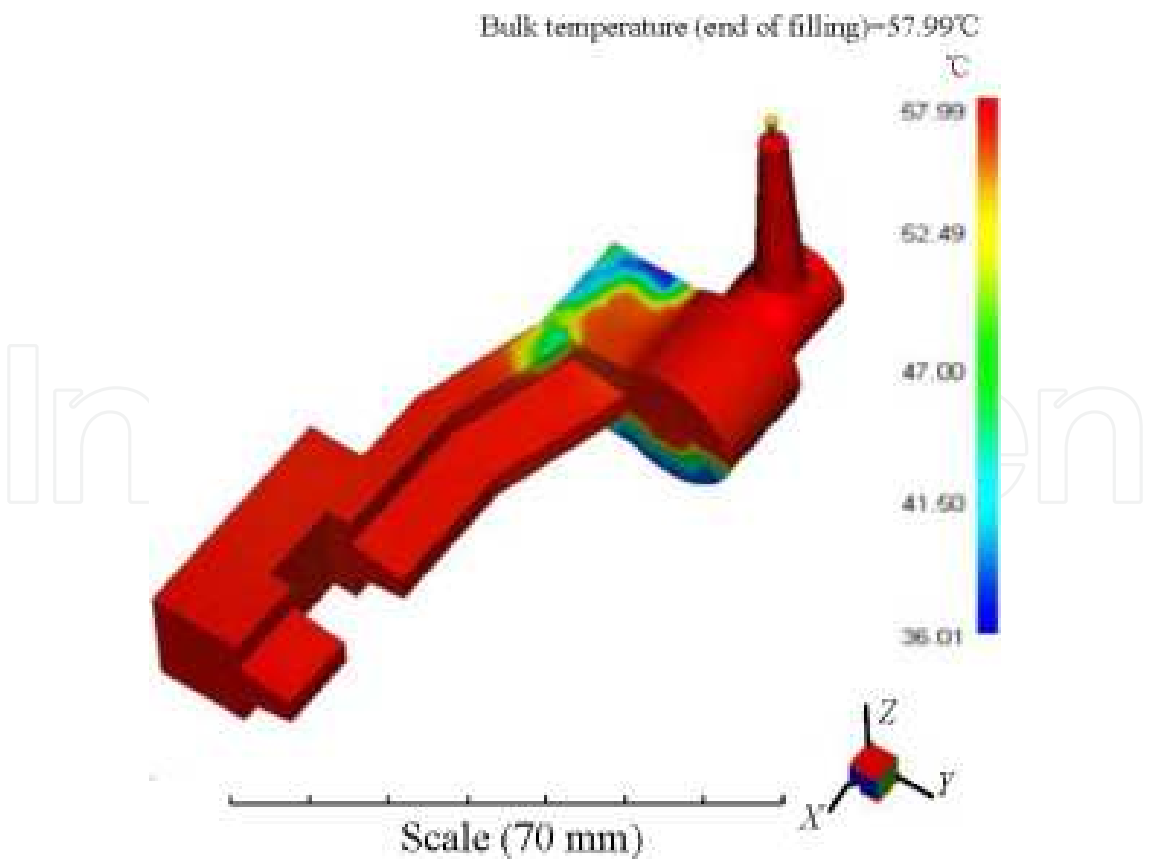


Fig. 19. Wax model temperature distribution

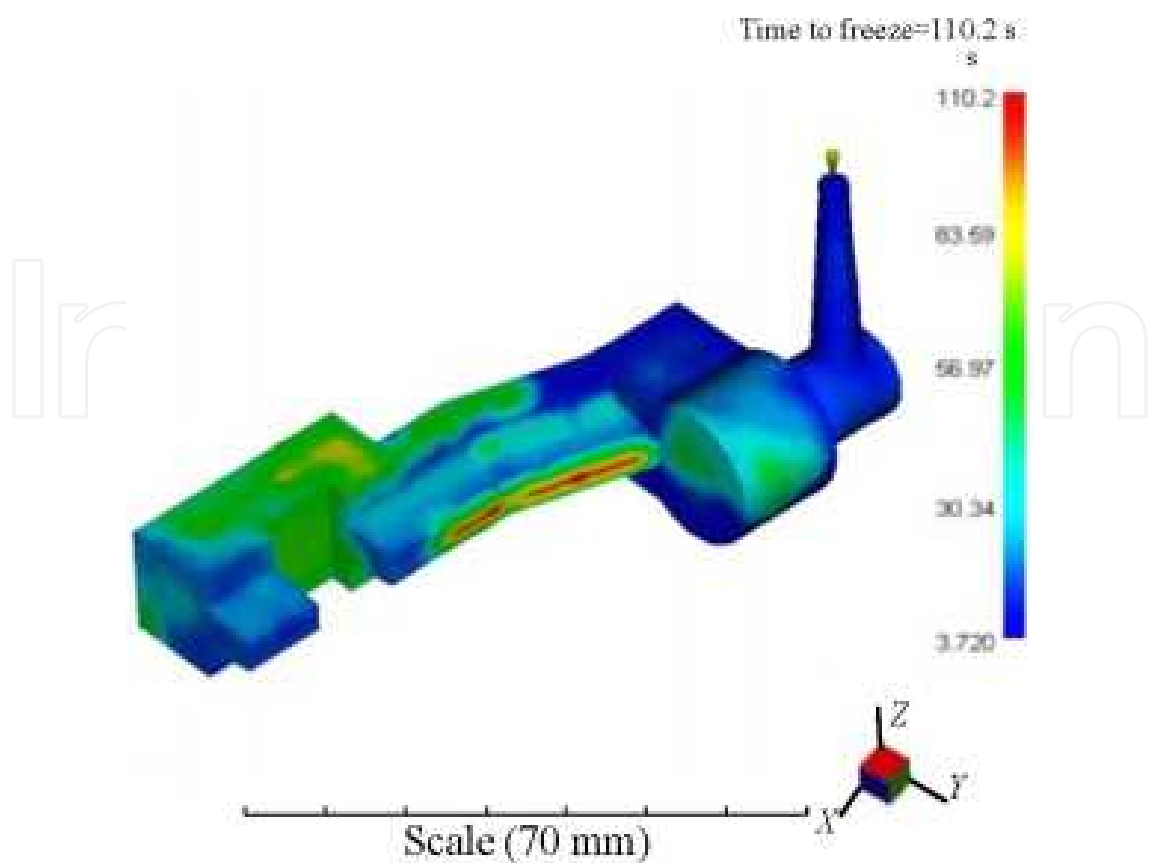


Fig. 20. Wax model freeze time

cavity was fabricated by photo-curable WaterShed 11120 resin with a 3-D SLA-5000™ machine (Fig. 21). Part layer thickness used in this process was 0.1 mm. After producing SLA inserts, post-processing operations such as washing excessive resin and removing supports were carried out, and finally core and cavity inserts were post cured in a UV oven. The final stage of post-processing operation was delicately finishing the inserts using a very fine sand paper.



Fig. 21. Fabricated inserts of Peugeot engine gearbox shift fork using stereolithography

To increase the tool mechanical stiffness, hardness, and precise tool alignment, and to minimize epoxy material consumption, a modular steel mould base was designed. Two standard base plates were machined into rectangular pocket to fit the inserts (Fig. 22). Base plates were machined using high speed milling machine to satisfy the required assembly tolerances. The inserts were then fitted into steel mould bases through steel frames, and back-filled with aluminum powder/aluminum chip/epoxy resin (Vantico 5052) mixture (Fig. 23).



Fig. 22. Base plate machined into a rectangular pocket



(a)



(b)

Fig. 23. Back-filling inserts along with copper cooling pipes

The vacuum casting machine (MCP 006) was used to vacuum the back-filled material to the desired pressure for an hour to ensure no bubbles would remain during back-filling process. In the mean time, to conduct away heat from the tool during wax injection, copper pipes were applied as shown in Fig. 23. The back-filled mixture added strength to the inserts and allowed heat to be conducted away through copper pipes and the mould. After the back-filled solidification occurred in ambient condition, the back-filled surface which is going to be in contact with the base plate was machined and grinded.

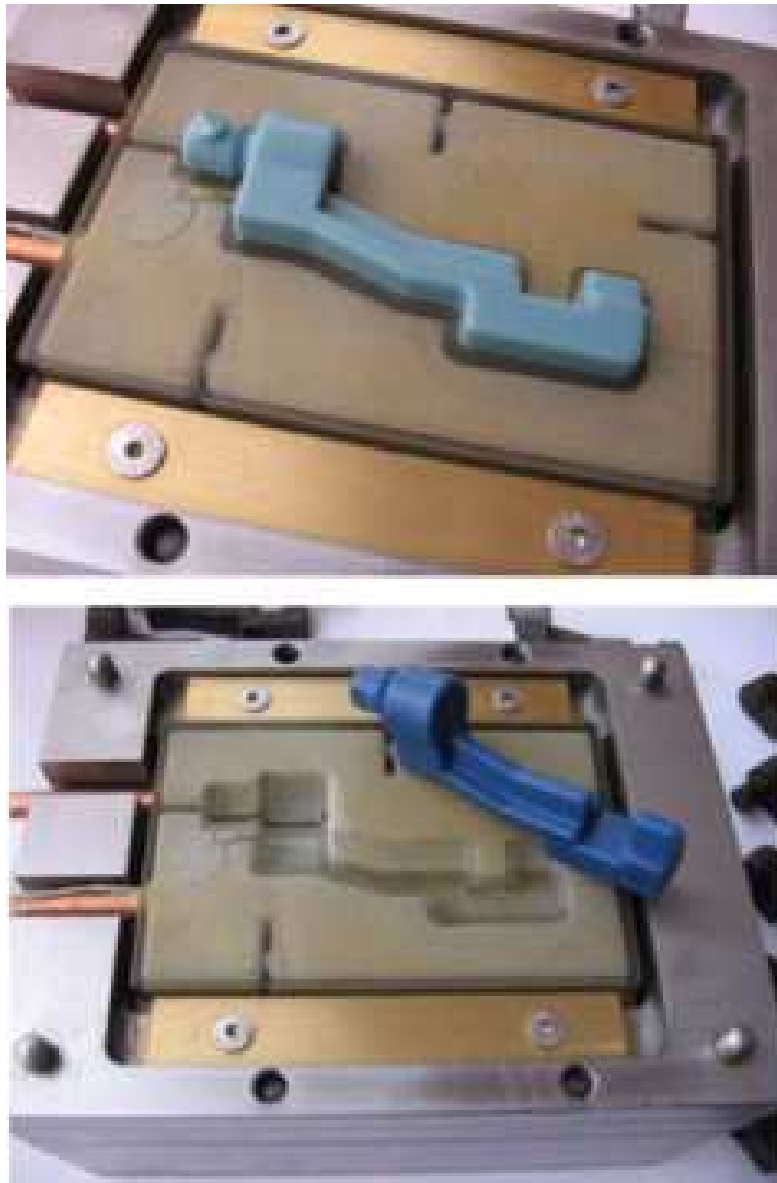


Fig. 24. Wax moulding of Peugeot engine gearbox shift fork

### 3.4 Wax tool injection process

During the initial moulding process, the wax injection test was carried out at SAPCO Co. manually, in such a way that two mould halves were held against each other using different holders and clamps. Then five shots of wax were injected at 80°C and at two bars pressure. Next, for the actual moulding process, the tool was taken to the POLADIR Investment Casting Company to produce final wax patterns. MV30 wax injection machine was used at vertical orientation and parameter settings were applied using the simulation analysis results.

During the moulding process, the temperature and pressure of the cavity was monitored, and the melt temperature was controlled using different thermocouples to ensure that the conditions within the cavity remains as consistent as possible. Finally, 100 shots of shift fork of Peugeot engine gearbox were made with wax melt temperature at 65°C and 5 bars pressure (Fig. 24).

3.5 Discussion

The rapid wax injection tool was successfully tested and the results revealed the success of the technique. Slim edges and sharp corners have been very well reflected on the wax model. This is specially highlighted when compared with traditional tooling which requires special attention while machining sharp corners. For example, during machining the traditional tools, the tool radius leads to undesirable fillets, which requires additional process such as EDM machining to trim such fillets into sharp corners. Any additional process means additional time and cost, probably sacrificing accuracy as well. During wax model production, in spite of the abrupt difference in heat conductivity coefficient between epoxy and steel tool, heat of wax melt was conducted well to the tool base and the cycle time had no significant change compared with traditional tooling. Temperature data regarding barrel and nozzle during injection process is given in Table 5. The proper tool design, with copper cooling pipes and continuous tool temperature monitoring using different thermocouples, has resulted in uniform cycle profiles as shown in Fig. 25. According to the present production rate, the tool has produced 100 shots in an hour versus 300 shots in an hour in traditional tooling, which seems to be acceptable. It is possible to improve this rate using multi-cavity tool, which makes this technique further suitable and economical for fast part production.

Nozzle	Barrel	Upper plate	Lower plate	Wax model
65	60	13	14	45

Table 5. Temperature settings during wax injection process (°C)

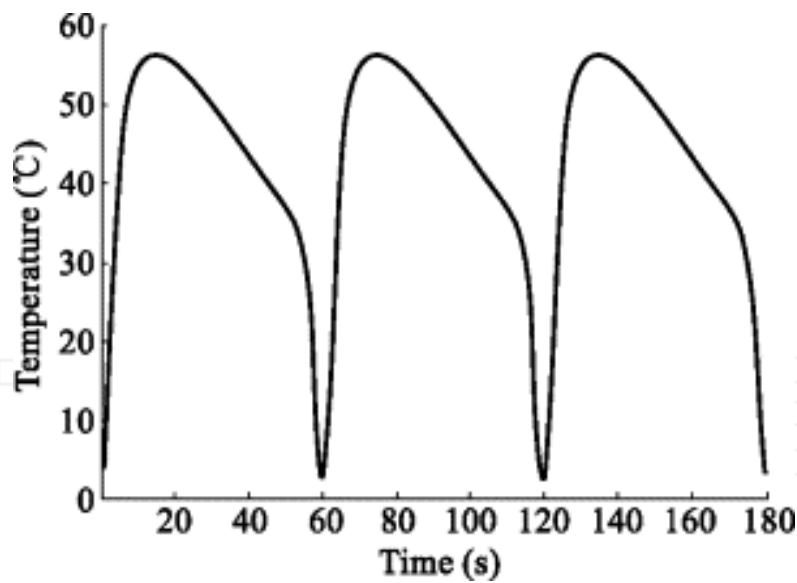


Fig. 25. Temperature changes at tool cavity surface versus time in consecutive cycles

In order to check the dimensional accuracy of the wax model, optical measuring system was applied to extract the interested dimensions. The standard deviation of the wax model was 0.08 mm (Fig. 15). The general tolerance of the wax model was found to be in the range of  $\pm 0.1$  mm, which was acceptable by the manufacturer. The nominal dimensions of the wax model are given at Table 6, and the actual dimensions of the produced wax model are given at Table 7.



$L_1$	$L_2$	$L_3$	$L_4$	$L_5$	$L_6$
77.8	62.42	15.38	11.99	11.33	45.1
$L_7$	$L_8$	$L_9$	$L_{10}$	$L_{11}$	$D_1$
32.7	21.12	9.74	8.2	15.38	19.47

Table 6. Wax model nominal dimensions (mm)

$L_1$	$L_2$	$L_3$	$L_4$	$L_5$	$L_6$
77.5	62.1	15.17	11.8	11.25	45.3
$L_7$	$L_8$	$L_9$	$L_{10}$	$L_{11}$	$D_1$
32.53	20.82	9.55	8.15	15.1	19.25

Table 7. Wax model actual dimensions (mm)

Comparing the results of Table 6 and Table 7, the largest difference belongs to  $L_1$  and  $L_3$ , which is 0.3 mm. These two parameters are located where they can have free shrinkage while other parameters have constraint in shrinkage. With respect to the thickness, except  $L_4$  which has 0.19 mm increase in thickness, the remaining parameters fit within the tolerance. Parameter  $L_{11}$  has shrinkage of 0.29 mm which is precisely equivalent to the forecasted value suggested by the simulation software (Fig. 26).

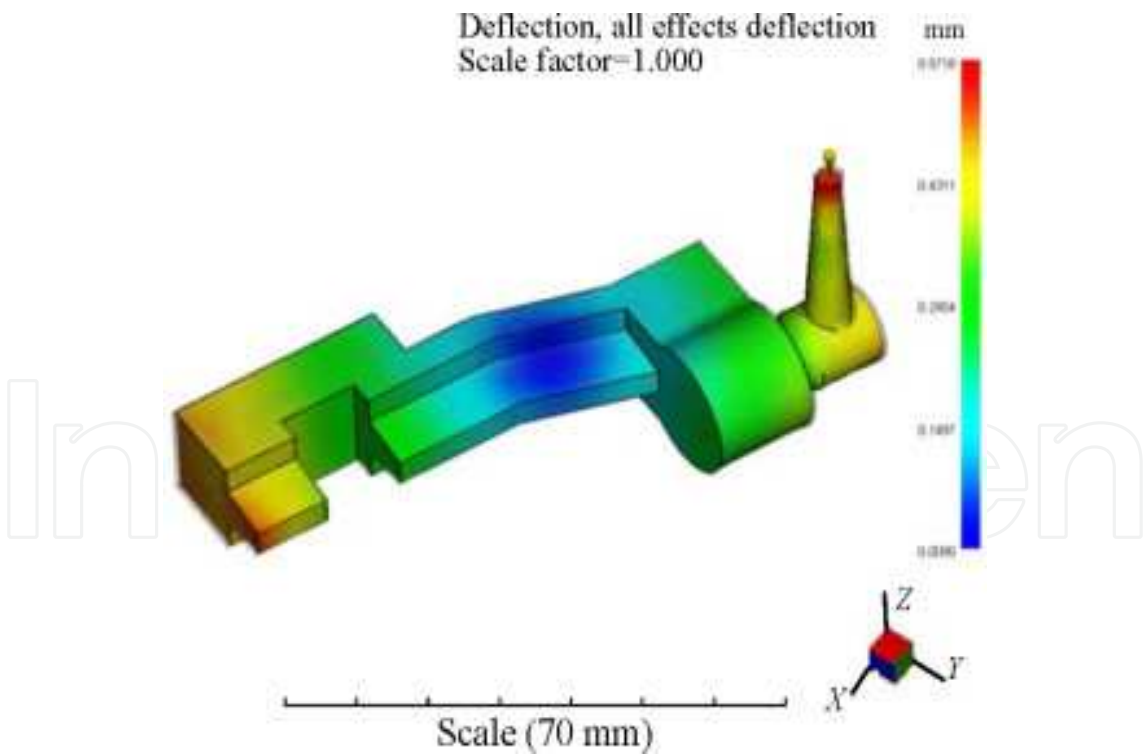


Fig. 26. Wax model warpage and shrinkage after ejection

Considering the difference between the nominal and actual dimensions, and with respect to the applied coefficient of shrinkage, it could be concluded that the tool cooling method has influence on the wax shrinkage (Modukuru et al., 1996). Moreover, those parameters which

reveal larger shrinkages have no constraint and can shrink freely. Therefore, the calculated shrinkage was found to be 1.5% in length and 2.5% in thickness, which is in accordance to the suggested values by the MoldFlow simulation software (Fig. 27).

Comparing the theoretical results of the simulation softwares with the actual results, confirms the reliability and validity of the investigation. With respect to the time and cost saving in applying wax rapid tooling compared to the traditional tooling, the time saving was 50% and the cost saving was 60%. This comparison takes into consideration parameters affecting the time and cost of tool design, manufacturing, and issues such as material recruitment, and other services for tool manufacturing in terms of instruments, human resources, and finishing operations.

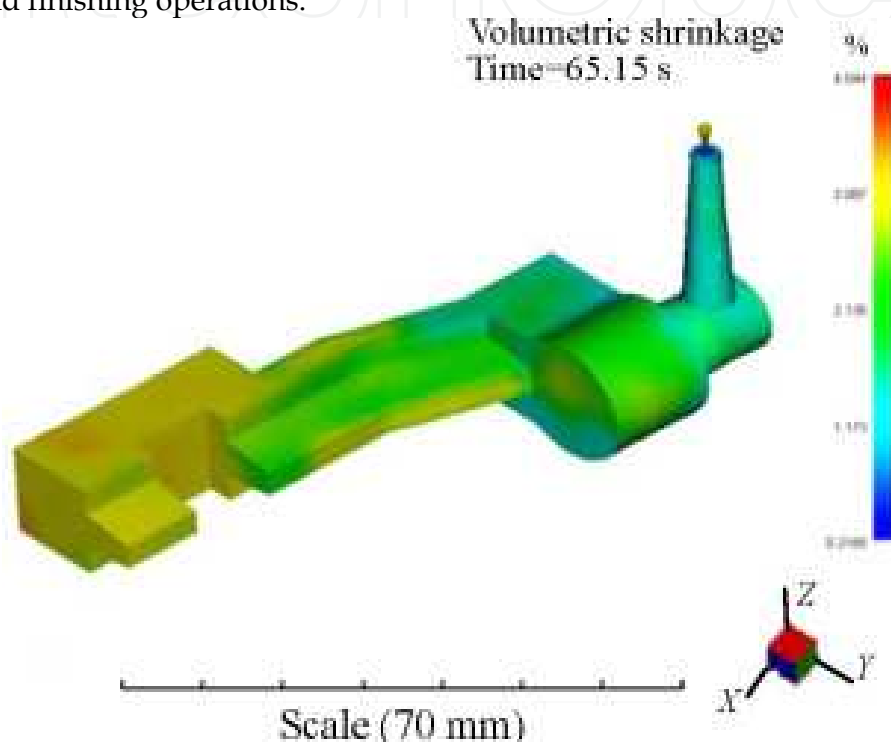


Fig. 27. Shrinkage at 10th second of wax injection

### 3.6 Summary

A rapid wax injection tool of a gearbox shift fork is designed, simulated, and manufactured using rapid prototyping and rapid tooling technology to save time and cost of producing wax models used for the investment casting process. CAE simulation softwares, in particular, MoldFlow, are used to get wax injection moulding parameters such as filling parameters, temperature profiles, freeze time, speed, and pressure. The results of this research were compared with conventional wax model production methods. The criteria of such comparison were based upon parameters such as time, cost, and other related characteristics, which resulted in saving of 50% in time and 60% in cost. In this research, design, assembly, and wax injection operation of the wax tool has taken 10 days. Considering the fact that wax melting temperature is as low as 70°C and injection pressure of 0.5 MPa, the tool suffers no damage due to the thermal and pressure stresses, leading to the mass production of wax models.

This research aimed at investigating the feasibility of applying rapid prototyping and rapid tooling technology into the wax model production for investment casting process. The

results not only confirm the success of such application, but also prove valuable benefits with respect to the common tooling techniques.

- Due to the fact that many moulding parameters inside the cavity such as pressure and melt temperature, are not easily possible to be measured; therefore, CAE simulation softwares are unique and inexpensive alternatives to analyze and evaluate such rapid tools.
- Obviously, CAE simulation softwares such as MoldFlow and ANSYS are significant aids in rapid tooling analysis, acquiring tooling parameters and melt behavior in the cavity; and today's rapid tooling analyses of different tooling techniques have been developed and are complementary.
- The results of this research indicate saving of 50% in time and 60% in cost. Design, assembly, and wax injection operation took 10 days, compared with the traditional techniques which may take at least two month.
- Considering the fact that wax melting temperature is as low as 70°C and injection pressure of 0.5 MPa, the tool may suffer no damage due to the thermal and pressure stresses, leading to the mass production of wax models.
- Using simulation softwares prevents common moulding defects well in advance before being encountered during operation.
- Injection cycle time is found to be between 40–50 sec which is longer than the common tooling techniques (5–15 sec), which is due to the fact that the tool cavity is a nonconductive material; however, this may be improved by increasing the number of cavities (multi cavity).
- Due to the modular nature of tool plate and frame assembly, it is possible to reuse the material for similar tool dimensions, leading to more saving in time and cost for new tools.
- According to the above findings, it could be concluded that the rapid wax injection tooling is an appropriate alternative for mass production via investment casting process. Therefore, rapid wax injection tooling technique could replace many expensive, time consuming, and complex machining techniques.

#### 4. Acknowledgment

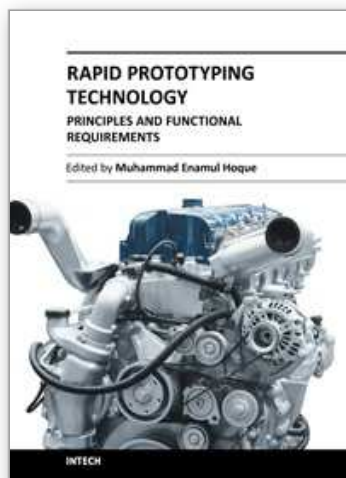
The author would like to thank the Islamic Azad University – Majlesi Branch, Rapid Prototyping & Tooling Branch of SAPCO Part Supplier of Car Manufacturing Co. of Iran-Khodro and POULADIR Investment Casting Company for supporting this project.

#### 5. References

- Bibb, et al. (2009). Rapid manufacture of custom-fitting surgical guides, *Rapid Prototyping Journal*, Vol. 15, No. 5, pp. 346–354, DOI: 10.1108/13552540910993879, ISSN 1355-2546.
- Bonilla, W.; Masood, SH. & Iovenitti, P. (2001). An investigation of wax patterns for accuracy improvement in investment cast parts, *The International Journal of Advanced Manufacturing Technology*, 18 (5), pp. 348–356, DOI: 10.1007/s001700170058, ISSN 0268-3768.

- Campbell, et al. (2011). Additive manufacturing in South Africa: building on the foundations, *Rapid Prototyping Journal*, Vol. 17, No. 2, pp. 156-162, DOI: 10.1108/13552541111113907, ISSN 1355-2546.
- Chen, D. & Cheng, F. (2000). Integration of Product and Process Development Using Rapid Prototyping and Work-Cell Simulation Technology, *Journal of Industrial Technology*, Vol. 16, No. 1.
- Decelles, P. & Barritt, M. (1996). Direct AIM Prototype Tooling, *3D Systems*, P/N 70275/11-25-96.
- Evans, M.A. & Campbell, R. I. (2003). A Comparative evaluation of industrial design models produced using Rapid Prototyping and workshop-based fabrication techniques. *Rapid Prototyping Journal*, Vol. 9, No. 5, DOI: 10.1108/13552540310502248, ISSN 1355-2546.
- Gargiulo, E.P. (1992). Stereolithography Process Accuracy; user experience. *Proceedings of 1st European conference on rapid prototyping*, pp. 187-201.
- Greaves, T. (1997). Case Study: Using Stereolithography to Directly Develop Rapid Injection Mold Tooling, (Delphi-GM), *TCT Conference*.
- Ilyas, et al. (2010). Design and manufacture of injection mould tool inserts, *Rapid Prototyping Journal*, Vol. 16, No. 6, pp. 429-440, DOI: 10.1108/13552541011083353, ISSN 1355-2546.
- Investment Casting Institute. (1968). *Investment Casting Handbook*. Chicago.
- Jacobs, P.F. (1992). *Rapid Prototyping and Manufacturing - Fundamentals of Stereolithography*, McGraw-Hill Inc, New York.
- Jacobs, P.F. (1996). Recent Advances in Rapid Tooling from Stereolithography, *A Rapid Prototyping Conference*, University of Maryland, USA.
- Menges, G. & Mohren, P. (1986). *How to Make Injection Molds*, Hanser, Munich.
- Modukuru, SC.; Ramakrishnan, N. & Sriramamurthy, AM. (1996). Determination of the die profile for the investment casting of aerofoil-shaped turbine blades using the finite-element, *Journal of Materials Processing Technology*, 58 (2-3), pp. 223-226, DOI:10.1016/0924-0136(95)02127-2.
- Rahmati, S. & Dickens, P.M. (1997). Stereolithography for Injection Mould tooling. *Rapid Prototyping Journal*, Vol. 3, No. 2, pp. 53-60, DOI: 10.1108/13552549710176671, ISSN 1355-2546.
- Rahmati, S., and Dickens, P. M., (2005) Stereolithography Rapid tooling for Injection Moulding, 2nd International Conference on Advanced Research in Virtual and Rapid Prototyping, Leiria, Portugal, Edited by Dr P.J. Bártolo et al., Taylor & Francis, ISBN 0-415-39062-1.
- Rauwendaal, Chris. (2000). Statistical Process Control in Injection Molding and Extrusion, *Hanser*, Munich, ISBN 3-446-18814-2.
- Richard, P. C. (1993). Material and Process Parameters that Affect Accuracy in Stereolithography, *Solid freeform fabrication proceedings*, pp. 245-252.
- Rosochowski, A. & Matuszak, A. (2000). Rapid tooling: The state of art, *Journal of Materials Processing Technology*, 106, pp. 191-198, DOI:10.1016/S0924-0136(00)00613-0.

- Quail, et al. (2010). Development of a regenerative pump impeller using rapid manufacturing techniques, *Rapid Prototyping Journal* , Vol. 16, No. 5, pp. 337-344, DOI: 10.1108/13552541011065731, ISSN 1355-2546.
- Siegfried, W. & Wadenius, B. (2000). The expansion/shrinkage behaviour of wax. *Report from J. F. Mccaughin Co.*
- Walter, M. & Helmut, G. (2000). Training in Injection, Molding, , *Hanser*, Munich, ISBN 10: 1-56990-302-6
- Weiss, et al. (1990). A Rapid Tool Manufacturing System Based on Stereolithography and Thermal Spraying, *ASME Manufacturing Review*, Vol. 3, pp. 40-48.



## **Rapid Prototyping Technology - Principles and Functional Requirements**

Edited by Dr. M. Hoque

ISBN 978-953-307-970-7

Hard cover, 392 pages

**Publisher** InTech

**Published online** 26, September, 2011

**Published in print edition** September, 2011

Modern engineering often deals with customized design that requires easy, low-cost and rapid fabrication. Rapid prototyping (RP) is a popular technology that enables quick and easy fabrication of customized forms/objects directly from computer aided design (CAD) model. The needs for quick product development, decreased time to market, and highly customized and low quantity parts are driving the demand for RP technology. Today, RP technology also known as solid freeform fabrication (SFF) or desktop manufacturing (DM) or layer manufacturing (LM) is regarded as an efficient tool to bring the product concept into the product realization rapidly. Though all the RP technologies are additive they are still different from each other in the way of building layers and/or nature of building materials. This book delivers up-to-date information about RP technology focusing on the overview of the principles, functional requirements, design constraints etc. of specific technology.

### **How to reference**

In order to correctly reference this scholarly work, feel free to copy and paste the following:

Sadegh Rahmati (2011). Rapid Tooling Development, Rapid Prototyping Technology - Principles and Functional Requirements, Dr. M. Hoque (Ed.), ISBN: 978-953-307-970-7, InTech, Available from: <http://www.intechopen.com/books/rapid-prototyping-technology-principles-and-functional-requirements/rapid-tooling-development>

**INTech**  
open science | open minds

### **InTech Europe**

University Campus STeP Ri  
Slavka Krautzeka 83/A  
51000 Rijeka, Croatia  
Phone: +385 (51) 770 447  
Fax: +385 (51) 686 166  
[www.intechopen.com](http://www.intechopen.com)

### **InTech China**

Unit 405, Office Block, Hotel Equatorial Shanghai  
No.65, Yan An Road (West), Shanghai, 200040, China  
中国上海市延安西路65号上海国际贵都大饭店办公楼405单元  
Phone: +86-21-62489820  
Fax: +86-21-62489821

© 2011 The Author(s). Licensee IntechOpen. This chapter is distributed under the terms of the [Creative Commons Attribution-NonCommercial-ShareAlike-3.0 License](https://creativecommons.org/licenses/by-nc-sa/3.0/), which permits use, distribution and reproduction for non-commercial purposes, provided the original is properly cited and derivative works building on this content are distributed under the same license.

IntechOpen

IntechOpen